

T_H2-Polarized CD4⁺ T Cells and Macrophages Limit Efficacy of Radiotherapy

Stephen L. Shiao¹, Brian Ruffell², David G. DeNardo³, Bruce A. Faddegon⁴, Catherine C. Park⁴, and Lisa M. Coussens²

Abstract

Radiotherapy and chemotherapy following surgery are mainstays of treatment for breast cancer. Although multiple studies have recently revealed the significance of immune cells as mediators of chemotherapy response in breast cancer, less is known regarding roles for leukocytes as mediating outcomes following radiotherapy. To address this question, we utilized a syngeneic orthotopic murine model of mammary carcinogenesis to investigate if response to radiotherapy could be improved when select immune cells or immune-based pathways in the mammary microenvironment were inhibited. Treatment of mammary tumor-bearing mice with either a neutralizing mAb to colony-stimulating factor-1 (CSF-1) or a small-molecule inhibitor of the CSF-1 receptor kinase (i.e., PLX3397), resulting in efficient macrophage depletion, significantly delayed tumor regrowth following radiotherapy. Delayed tumor growth in this setting was

associated with increased presence of CD8⁺ T cells and reduced presence of CD4⁺ T cells, the main source of the T_H2 cytokine IL4 in mammary tumors. Selective depletion of CD4⁺ T cells or neutralization of IL4 in combination with radiotherapy phenocopied results following macrophage depletion, whereas depletion of CD8⁺ T cells abrogated improved response to radiotherapy following these therapies. Analogously, therapeutic neutralization of IL4 or IL13, or IL4 receptor alpha deficiency, in combination with the chemotherapy paclitaxel, resulted in slowed primary mammary tumor growth by CD8⁺ T-cell-dependent mechanisms. These findings indicate that clinical responses to cytotoxic therapy in general can be improved by neutralizing dominant T_H2-based programs driving protumorigenic and immune-suppressive pathways in mammary (breast) tumors to improve outcomes. *Cancer Immunol Res*; 3(5); 518–25. ©2015 AACR.

Introduction

Breast cancer is the most prevalent malignant disease of women in the developed world and remains one of the leading causes of death (1). Radiation and chemotherapy form the mainstay of treatment for patients with breast cancer, and more than half of all patients diagnosed with breast cancer will receive some form of radiotherapy (2). Although the antitumor properties of radiotherapy have long been considered a neoplastic cell-intrinsic process, evidence from multiple murine tumor models has demonstrated a critical role for immune cells in mediating radiotherapy response (3–6). Although much of the immune response against tumors has been attributed to T cells, myeloid cell bioactivity is also altered by radiotherapy and can regulate response to therapy (5, 6).

The presence of macrophages in multiple types of human cancer, including breast, ovarian, non-small cell lung cancer, mesothelioma, and Hodgkin lymphoma, correlates with poor clinical outcome, and it was associated with the ability of macrophages to enhance angiogenesis and promote the invasive and metastatic potential of malignant cells (7–11). The cytokine colony-stimulating factor (CSF)-1 plays a key role in recruitment and activation of macrophages following interaction with the CSF-1 receptor (CSF-1R), a high-affinity transmembrane receptor tyrosine kinase (12). Accordingly, in human breast cancer, colon cancer, and leiomyosarcoma, a CSF-1-response gene signature has been identified that predicts the risk of recurrence and metastasis (13–15). The ability to preferentially target macrophages via inhibiting the CSF-1/CSF-1R signaling pathway has led to several preclinical studies demonstrating therapeutic efficacy in glioblastoma; melanoma; and mammary, prostate, pancreas, and cervical carcinoma, either in combination with chemotherapy and radiotherapy or as monotherapy (16–20).

We and others have previously described a transgenic mouse model of aggressive mammary adenocarcinoma development in which late-stage carcinogenesis and pulmonary metastasis are regulated by CSF-1, tissue macrophages, and IL4-producing CD4⁺ T cells (21–23). Using this model, we recently reported that when macrophage infiltration into tumors was minimized via blockade of the CSF-1/CSF-1R pathway, platinum and paclitaxel-based chemotherapy responses were improved in a CD8⁺ T-cell-dependent manner (16) regulated by IL12-expressing dendritic cells (24). Based on these studies, we hypothesized that response to radiotherapy, like response to chemotherapy, could be improved by either reducing the presence of macrophages in tumors or by blocking induction of their T_H2 polarization. Herein, we report

¹Department of Radiation Oncology, Cedars-Sinai Medical Center, Los Angeles, California. ²Department of Cell, Developmental and Cancer Biology and Knight Cancer Institute, Oregon Health and Science University, Portland, Oregon. ³Department of Medicine, Department of Pathology and Immunology, and Siteman Cancer Center, Washington University School of Medicine, St. Louis, Missouri. ⁴Department of Radiation Oncology, Helen Diller Family Comprehensive Cancer Center, University of California, San Francisco, San Francisco, California.

Note: Supplementary data for this article are available at Cancer Immunology Research Online (<http://cancerimmunolres.aacrjournals.org/>).

Corresponding Author: Lisa M. Coussens, Knight Cancer Institute, Oregon Health and Science University, 181 SW Sam Jackson Park Road, Portland, OR 97239-3098. Phone: 503-494-7811; Fax: 503-494-4253; E-mail: coussenl@ohsu.edu

doi: 10.1158/2326-6066.CIR-14-0232

©2015 American Association for Cancer Research.

that regrowth of mammary tumors following radiotherapy correlates with influx of T_H2-polarized macrophages and inhibiting macrophage recruitment after radiotherapy by neutralizing CSF-1 or blocking CSF-1R kinase activity significantly slows tumor regrowth. Moreover, our data indicate that radiotherapy promotes T_H2 polarization of infiltrating IL4-expressing CD4⁺ T cells, and that either depleting these or neutralizing IL4 slows tumor regrowth following radiotherapy, thus demonstrating that therapeutic targeting of T_H2 cytokines and the myeloid cells they regulate can enhance response to cytotoxic therapy.

Materials and Methods

Preclinical mouse models and animal husbandry

FVB/n strain background mice harboring the polyoma middle T (PyMT) transgene under the control of the mouse mammary tumor virus (MMTV) promoter have been described previously (23, 25). To generate a syngeneic orthotopic implantable tumor model, we prepared single-cell suspensions of tumor cell pools isolated from mammary tumors of 100-day-old MMTV-PyMT mice, and injected 1.0 million (total) tumor cells diluted in medium and basement membrane extract (Matrigel; BD Pharmingen) orthotopically into unexcised mammary fat pads (4th gland) of 10-week-old virgin FVB/n female mice (16). Following implantation, tumors were allowed to grow to an average diameter of 1.0 cm before randomization and enrollment into studies. Mice were randomized into treatment groups, e.g., PLX3397, α CSF-1 mAb (5A1), α CD4 mAb (GK1.5), α CD8 (YTS169.4), or α IL4 mAb (11B11), based on tumor size and subsequently irradiated with a single fraction of 5 Gy focal gamma irradiation (Mark III Cesium Irradiator) generated from a cesium source with mice mounted in a custom shielding apparatus (Fig. 1A). PLX3397 (16) was formulated in mouse chow so that the average dose per animal per day was 40 mg/kg, and chow containing vehicle alone was used as a control. Antibodies were injected i.p. at 1.0 mg to start, followed by 500 μ g every 5 days. Depletion of CD4⁺ and CD8⁺ cells was confirmed by flow cytometry of peripheral blood before initiating therapy. Pharmaceutical grade paclitaxel (Hospira) was administered i.v. every 5 days at 10 mg/kg as described (16, 24). Neutralization of IL13 was achieved via administration of a rat anti-mouse IL13 mAb (54D1) injected i.p. at 1.0 mg to start, followed by 500 μ g every 5 days. Tumor burden was evaluated by caliper measurement on anesthetized mice every 2 to 5 days. Before tissue collection, mice were cardiac perfused with PBS to clear peripheral blood. As described previously (23), homozygous null *IL4R α* mice were obtained from The Jackson Laboratories. To generate *PyMT* mice on the *IL4R α* ^{-/-} backgrounds, *IL4R α* ^{+/-} mice were backcrossed into the FVB/n strain to N6 and then intercrossed with *PyMT* mice to generate breeding colonies. Mice were maintained either within the University of California, San Francisco Laboratory for Animal Care barrier facility or the Oregon Health and Science University Department of Comparative Medicine barrier facility. Experiments involving animals were approved by the Institutional Animal Care and Use Committees at the respective institutions.

Flow cytometry analysis

Single-cell suspensions were prepared from mammary tumors disassociated by manual mincing and enzymatic digestion for 40 minutes at 37°C using collagenase A (3.0 mg/mL; Roche) and DNase I (Roche) dissolved in DMEM (Invitrogen) under stirring conditions. Digestion mixtures were quenched by adding DMEM

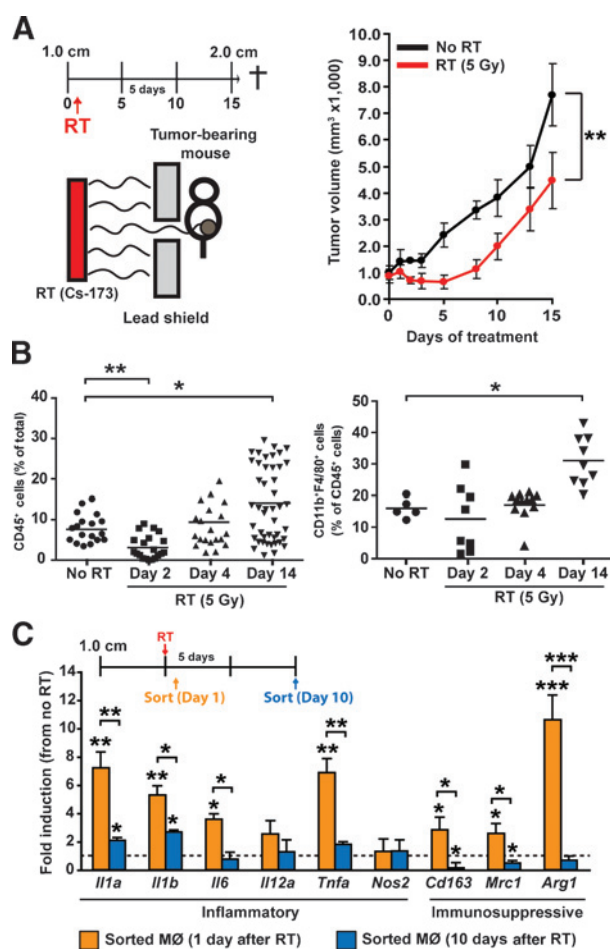


Figure 1. Macrophage recruitment and polarization following radiotherapy (RT). A, orthotopic MMTV-PyMT-derived explant tumors were grown to a median diameter of 1.0 cm, at which time tumor-bearing mice were enrolled in the experiment. One day later, the mice received localized gamma irradiation (5 Gy), and total tumor burden/animal was then assessed every 3 days until endpoint. Treatment schematic is depicted at top, and data are displayed as mean tumor burden \pm SEM (>8 mice/group). Statistical significance was determined by two-way ANOVA. One of two experiments is shown. B, quantification of CD45⁺ (left) and CD11b⁺F4/80⁺ (right) cells in mammary tumors on day 2, 4, and 14 following radiotherapy (5 Gy) compared with unirradiated tumors harvested on day 14. Data are depicted as mean number of CD45⁺ cells as a percentage of total cells \pm SEM as analyzed by flow cytometry (>5 mice/group). Statistical significance was determined by an unpaired *t* test. C, CD45⁺CD11b⁺F4/80⁺ macrophages (M ϕ) were FACS sorted from orthotopic PyMT-derived tumors at days 1 and 10 following radiotherapy (5 Gy). mRNA expression from sorted cells was analyzed using quantitative real-time PCR for the indicated genes. Treatment schematic is depicted at top, and data are expressed as mean fold change \pm SD compared with untreated tumors (4 mice/group). Statistical significance was determined by an unpaired *t* test relative to untreated controls, or between days 1 and 10 as indicated. For all panels, statistical significance is shown as follows: *, *P* < 0.05; **, *P* < 0.01; ***, *P* < 0.001.

containing 10% FBS and then filtered through 0.7- μ m nylon strainers (Falcon). Cells were then incubated for 10 minutes at 4°C with rat anti-mouse CD16/CD32 mAb (BD Biosciences) at a 1:100 dilution in PBS containing 1.0% of BSA (Sigma) to prevent nonspecific antibody binding. Subsequently, cells were washed

Shiao et al.

twice in PBS/BSA and incubated for 20 minutes with 100 μ L of fluorophore-conjugated anti-mouse antibodies: B220 (RA3-6B2), CD3e (145-2C11), CD4 (6K1.5), CD8 α (53-6.7), CD11b (M1/70), CD11c (N418), CD14 (Sa2-8), CD19 (MB19-1), Ly6C (HK1.4), Ly6G (1A8), CD44 (IM7), CD45 (30-F11), CD80 (16-10A1), CD86 (GL1), CD115 (AFS98), F4/80 (BM8), and/or MHCII (M5/114.15.2; all from eBioscience) followed by two washes with PBS/BSA. 7-AAD (BD Biosciences) was added (1:10) to discriminate between viable and dead cells, or alternatively live/dead aqua was used (Invitrogen). Data acquisition and analysis were performed on a LSRII (BD Biosciences) using the FlowJo version 8.8 software (Tree Star).

Immune cell isolation

Immune cells were isolated from tumors using a dual-purification strategy, including magnetic purification followed by flow sorting. Single-cell suspensions from tumors were generated as described above. Cells were incubated for 10 minutes at 4°C with rat anti-mouse CD16/CD32 mAb (BD Biosciences) at a 1:100 dilution in PBS/BSA and then washed twice in PBS/BSA and incubated for 20 minutes with appropriate fluorescent primary antibodies that included CD45-APC (30-F11), in addition to CD4 (GK1.1), CD3 (145-2C11), Gr-1 (RB6-8G5), CD11b (93), and/or F4/80 (BM8; all from eBiosciences) at 1:100 dilution depending on the population to be isolated. Total leukocytes were isolated using magnetic bead selection for CD45-APC⁺ cells according to the manufacturer's specifications (Miltenyi Biotec). Magnetically selected cells were then flow sorted on a FACSAria using FACSDiva software (BD Biosciences). Gating strategies for these populations have been described previously (16, 24).

Quantitative RT-PCR

Total tissue RNA was extracted from cells using an RNeasy Mini kit (QIAGEN). cDNAs were synthesized using Superscript III first-strand synthesis (Invitrogen). Primers specific for β -actin, GAPDH, 18S, IFN γ , IL2, IL4, IL12p35, IFN α , ARG1, and IL34 (Superarray) were used, and relative gene expression was determined using RT2 Real-Time SYBR Green/ROX PCR master mix (Superarray) on an ABI 7900HT quantitative PCR machine (ABI biosystems). Data were normalized to β -actin and GAPDH and/or 18S as reference genes. Alternatively, real-time PCR for gene expression was performed using individual TaqMan Assays following a preamplification step (Life Technologies), and data normalized to *Tbp* expression. The comparative threshold cycle method was used to calculate fold change in gene expression for all experiments.

Results

CSF-1/CSF-1R blockade delays primary tumor regrowth following radiotherapy

Using a syngeneic orthotopic murine explant model of mammary carcinoma growth, we first evaluated varying doses of radiation for effects on tumor growth and immune composition. Similar regression kinetics were observed following a single dose of 2, 5, or 8 Gy (Fig. 1A; Supplementary Fig. S1A); however, only 5 Gy provided a sufficient dose to induce a period of tumor stasis, followed by tumor regrowth approximately 8 to 12 days later (Fig. 1A). Analysis of immune infiltrates in mammary tumors at distinct time points following radiotherapy revealed reduced presence of CD45⁺ cells immediately following radiotherapy (day 2), with infiltration restored shortly thereafter (day 4), and

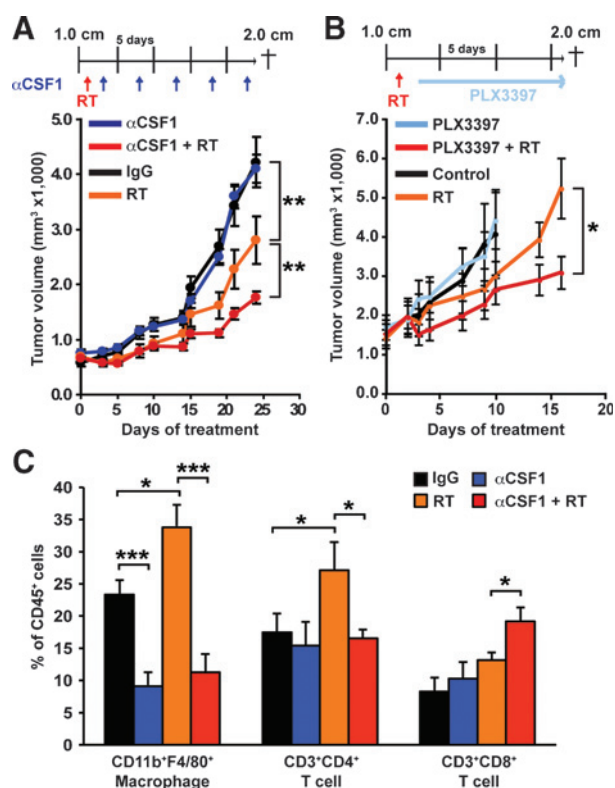


Figure 2.

Macrophage depletion following radiotherapy (RT) slows tumor regrowth. A and B, orthotopic PyMT-derived explant tumors were grown to a median diameter of 1.0 cm, and then the mice were enrolled in the study. On day 1, mice were subjected to localized gamma irradiation (5 Gy), and 2 days later treated with either α CSF-1-neutralizing mAb (A) or PLX3397 (B). mAb or PLX3397 was administered for a further 14 or 21 days, and total tumor burden/animal was assessed every 2 to 3 days. Treatment regimens are depicted for all cohorts, and data are displayed as mean tumor burden \pm SEM (>5 mice/group). Statistical significance was determined by two-way ANOVA. One of two experiments is shown. C, number of CD3⁺CD4⁺, CD3⁺CD8⁺, and CD11b⁺F4/80⁺ cells within tumors 17 days following radiotherapy in groups that were untreated, treated with α CSF-1 mAb alone, treated with radiotherapy (5 Gy) alone, or treated with a combination of radiotherapy and α CSF-1 mAb. Data are depicted as mean number of cells \pm SEM as a percentage of CD45⁺ cells as analyzed by flow cytometry (>5 mice/group). For all figures, statistical significance is shown as follows: *, $P < 0.05$; **, $P < 0.01$; ***, $P < 0.001$.

markedly elevated 2 weeks later (day 14; Fig. 1B). Although CD11b⁺F4/80⁺ macrophage infiltration was not altered during tumor regression (day 2) or stasis (day 4), macrophages were significantly increased during the tumor regrowth phase (day 14), even as compared with untreated tumors growing at a similar rate (Fig. 1B). Macrophages were also significantly increased on day 14 by 8 Gy, but not by 2 Gy radiation (Supplementary Fig. S1B). Gene expression analysis of infiltrating macrophages revealed increased acute expression of biomarkers, representing both classically and alternatively activated macrophages after radiotherapy, that returned to baseline as tumors initiated regrowth around day 10 (Fig. 1C), thus indicating that one consequence of acute radiotherapy is altered gene expression programs in resident leukocytes.

In a previous study, we reported that radiotherapy promotes CSF-1 expression by MMTV-PyMT-derived mammary epithelial

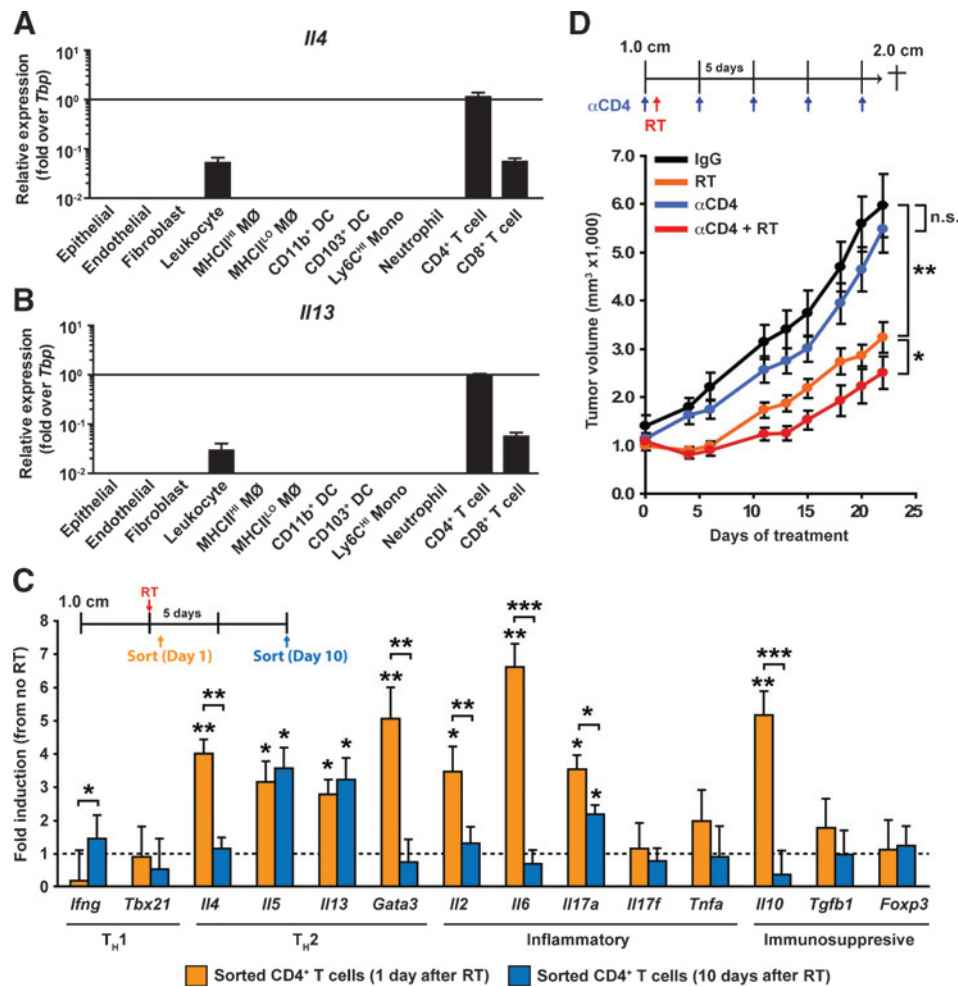


Figure 3.

T_H2-polarized CD4⁺ T cells promote tumor regrowth after radiotherapy (RT). A and B, mRNA levels of *Il4* (B) and *Il13* (C) in FACS-sorted populations of epithelial and stromal populations from untreated MMTV-PyMT mammary tumors, as determined by real-time PCR. Data are normalized to *Tbp* expression and displayed as mean ± SEM with $n = 8$ per cell type. DC, dendritic cell; MØ, macrophage; mono, monocyte. C, CD45⁺CD3⁺CD4⁺ T cells were FACS sorted from orthotopic PyMT-derived explant tumors at days 1 and 10 following radiotherapy (5 Gy). mRNA expression from sorted cells was then analyzed using quantitative real-time PCR for the indicated genes. Treatment schematic is depicted at the top, and data are expressed as mean fold change ± SD compared with untreated tumors (4 mice/group). Statistical significance was determined by an unpaired *t* test relative to untreated controls, or between days 1 and 10 as indicated. D, orthotopic PyMT-derived explant tumors were grown to a median diameter of 1.0 cm, and then the tumor-bearing mice were enrolled in the study. On day 1, mice were subjected to localized gamma irradiation (5 Gy), and total tumor burden/animal assessed every 3 days until endpoint. αCD4-depleting antibody was administered 2 days before radiotherapy and then every 5 days for the duration of the study. Treatment schematic is depicted at top, and data are displayed as mean tumor burden ± SEM (>8 mice/group). Statistical significance was determined by two-way ANOVA. One of two experiments is shown. For all figures, statistical significance is shown as follows: *, $P < 0.05$; **, $P < 0.01$; ***, $P < 0.001$.

cells *in vitro* (16); herein, we sought to evaluate whether delivery of immunologic or pharmacologic agents neutralizing the CSF-1/CSF-1R pathway could provide a therapeutic benefit to radiotherapy. To address this question, mice bearing syngeneic orthotopic mammary explant tumors were treated with either a neutralizing mAb against CSF-1 (clone 5A1) or a competitive ATP inhibitor selective for CSF-1R and cKIT receptor tyrosine kinases (PLX3397) currently being evaluated clinically (16, 20, 26, 27) 2 days following radiotherapy. Importantly, as low-dose radiotherapy has been reported to promote T-cell responses via macrophage repolarization (28), we initiated treatment 2 days following radiotherapy, with full depletion of macrophages anticipated approximately 3 days later (17). Treatment of mice with either αCSF-1 mAb (Fig. 2A) or PLX3397 (Fig. 2B) resulted in

significantly delayed/slowed tumor regrowth following radiotherapy, with no effect observed with either agent as monotherapy. Similar to our previous findings with these agents when delivered in combination with chemotherapy (16), the majority of tumor-infiltrating macrophages were efficiently eliminated by αCSF-1 mAb or PLX3397, and this was associated with an approximately 2-fold increase in CD8⁺ T-cell presence (Fig. 2C; Supplementary Fig. S2).

T_H2-polarized CD4⁺ T cells promote tumor regrowth after radiotherapy

Macrophage depletion, in combination with radiotherapy, was also associated with a substantial reduction in the presence of CD4⁺ T cells (Fig. 2C; Supplementary Fig. S2). This result was in

Shiao et al.

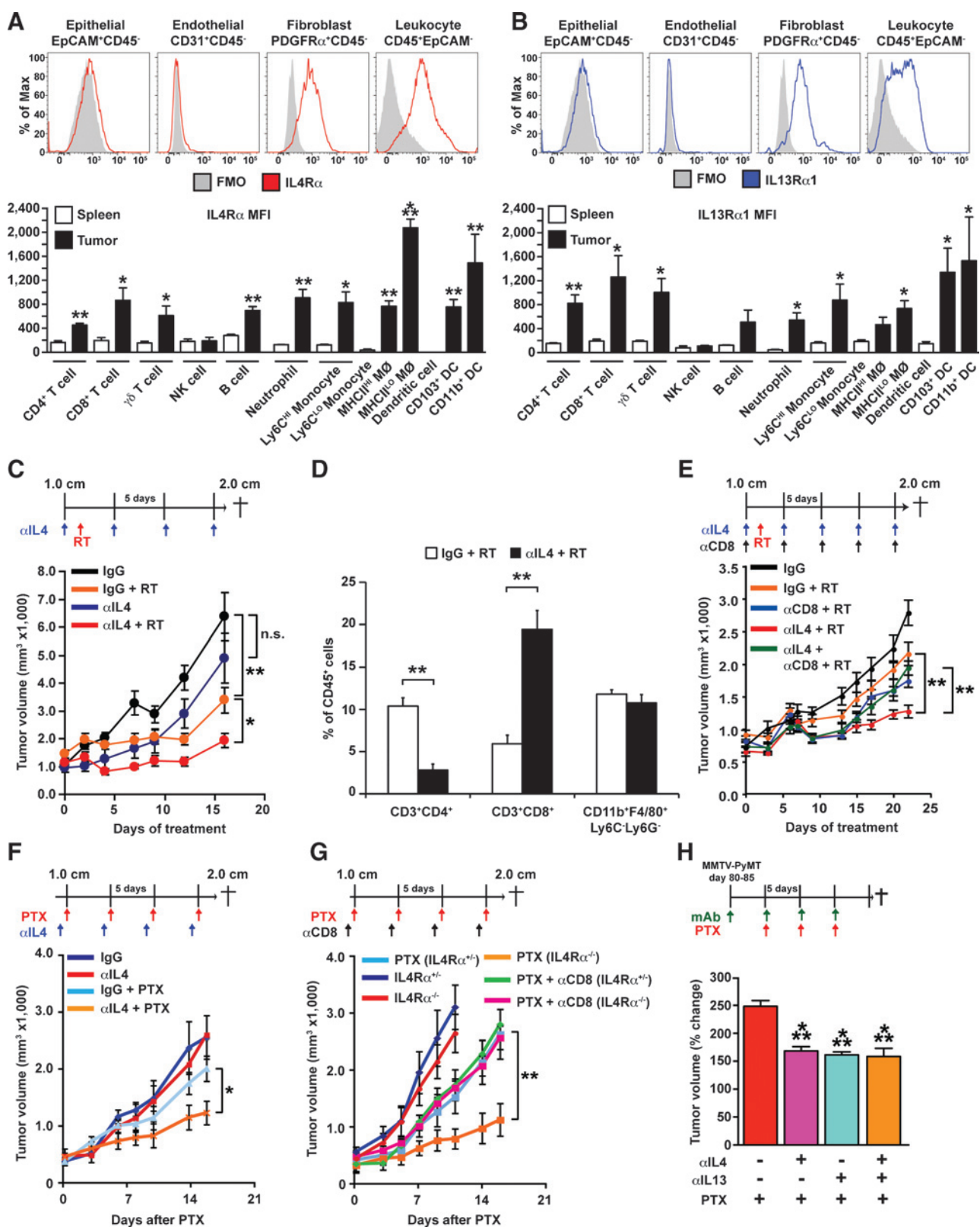


Figure 4. IL4 blockade slows tumor regrowth following radiotherapy (RT) in a CD8⁺ T-cell-dependent manner. A and B, surface expression of IL4Rα (A) and IL13Rα1 (B) as measured by mean fluorescence intensity (MFI) minus background in cells isolated from MMTV-PyMT mammary tumors as indicated, and as compared with equivalent populations in the spleens of non-tumor-bearing animals (lower graphs). (Continued on the following page.)

contrast with our previous findings in which CD4⁺ T-cell infiltration was unaffected by CSF-1/CSF-1R blockade as monotherapy, or in combination with chemotherapy (16, 24). That said, others have reported that a consequence of radiotherapy is altered expression of macrophage-expressed chemokines regulating T-cell infiltration in radiation-induced pneumonitis (29). In agreement with our previous results (16), CD4⁺ T cells in mammary tumors of MMTV-PyMT mice were main sources of IL4 (Fig. 3A) and IL13 (Fig. 3B), which are both significant cytokines regulating macrophage polarization. We therefore examined gene expression profiles of CD4⁺ T cells from mammary tumors by FACS-sorting cells 1 and 10 days after radiotherapy. We found that mRNA for T_H2 cytokines, including IL4, IL5, and IL13, and the T_H2 transcription factor GATA-3, were elevated at least 3-fold on day 1 after radiotherapy, with levels of IL5 and IL13 persisting to day 10 during tumor regrowth (Fig. 3C). Levels of IL2, IL6, and IL10 were also significantly induced, although these were not sustained (Fig. 3C); thus, radiotherapy induces significant gene expression changes in CD4⁺ T cells, in addition to macrophages (Fig. 1C).

To evaluate the functional significance of these findings and to determine if CD4⁺ T cells might also play a critical role in promoting tumor growth after radiotherapy, we administered an α CD4-depleting mAb to deplete CD4⁺ T cells before radiotherapy and then evaluated tumor regrowth; whereas CD4 depletion had no significant influence on tumor growth in untreated animals, tumor regrowth following radiotherapy was significantly diminished when CD4⁺ T cells were absent (Fig. 3D).

IL4 neutralization enhances antitumor immunity in response to radiotherapy

Based on these data, we next sought to evaluate the efficacy of neutralizing IL4 to determine if suppression of its T_H2-polarizing effects on immune and/or nonimmune cells influenced tumor growth and/or response to radiotherapy. IL4 and IL13 bind multimeric scaffold receptors composed of IL4R α , γ c (CD132), IL13R α 1, or IL13R α 2 subunits; type I receptors (IL4R α / γ c) are activated exclusively by IL4, whereas both IL4 and IL13 bind type II receptors (IL4R α /IL13R α 1; ref. 30). In mammary tumors of MMTV-PyMT mice, both receptor types are broadly expressed by immune cells infiltrating tumors, as well as by fibroblasts (Fig. 4A and B). Increased IL4R α was particularly pronounced in the MHCII^{LO} subset of macrophages (Fig. 4A), which are known to exhibit enhanced tumor-promoting properties (24, 31).

Neutralization of IL4 following radiotherapy significantly slowed tumor regrowth following radiotherapy as compared with either radiotherapy or α IL4 mAb alone (Fig. 4C), similar to CSF-1/CSF-1R blockade and CD4 depletion (Figs. 2 and 3). Analysis of the immune composition of tumors following α IL4 mAb/radiotherapy similarly revealed a significantly decreased presence of CD4⁺ T cells and significantly increased CD8⁺ T cells in the tumor parenchyma (Fig. 4D), which was significant as CD8⁺ T-cell depletion before radiotherapy abrogated improved responses (Fig. 4E), similar to the responses following CSF-1/CSF-1R blockade (16, 24). To determine if this improved response extended to chemotherapy, we evaluated mammary tumor growth in syngeneic IL4R α -deficient mice and wild-type mice treated with α IL4 mAb, with and without paclitaxel, and found significantly reduced primary tumor growth as compared with mice treated with paclitaxel or α IL4 mAb alone (Fig. 4F and G). Improved responses to paclitaxel were similarly dependent on induced CD8⁺ T-cell infiltration (Fig. 4G). Because IL4R α acts as a receptor for both IL4 and IL13, we also evaluated the effects of IL13 neutralization and found that α IL4 and α IL13 mAb produced equivalent effects on *de novo* mammary adenocarcinoma growth in combination with paclitaxel in transgenic MMTV-PyMT mice, with no additive effects observed when α IL4/ α IL13 were used in combination (Fig. 4H).

Discussion

Results reported herein from our study using a murine orthotopic explant model of primary mammary carcinoma reveal that a consequence of radiotherapy is induced recruitment of immunosuppressive F4/80⁺ macrophages that limit radiotherapy (and chemotherapy) efficacy. Recruitment of these protumorigenic immune cells is in part due to increased expression of CSF-1 and IL34 by mammary epithelial cells following cellular "damage" induced by radiotherapy (and chemotherapy) observed in both murine mammary models and clinical breast tumors following therapy (16, 32). Selective macrophage depletion resulting from CSF-1/CSF-1R blockade improved responses to radiotherapy and was associated with decreased presence of type 2 cytokine-expressing CD4⁺ T cells. Whether macrophages are directly responsible for CD4⁺ T-cell recruitment is unclear; that said, in other studies, we reported that therapeutically blocking humoral-based pathways regulating protumoral macrophage programming, in combination with chemotherapy, induced T_H1-type programming of

(Continued.) Data are displayed as mean \pm SEM with $n = 3$ mice per group. Statistical significance was determined by an unpaired *t* test compared with the spleen. DC, dendritic cell. M ϕ , macrophage; mono, monocyte. C and D, orthotopic PyMT-derived tumors were grown to a median diameter of 1.0 cm, and then the tumor-bearing mice were enrolled in the study. On day 1, mice were treated with localized gamma irradiation (5 Gy), and total tumor burden/animal assessed every 3 days until endpoint. α IL4-neutralizing antibody and/or α CD8-depleting antibody were administered 2 days before radiotherapy and then every 5 days for the duration of the experiment. Treatment schematic is depicted at top, and data are displayed as mean tumor burden \pm SEM (>5 mice/group). Statistical significance was determined by two-way ANOVA. E, number of CD3⁺CD4⁺, CD3⁺CD8⁺, and CD11b⁺F4/80⁺ cells within tumors 2 days following radiotherapy. Data are depicted as mean number of cells \pm SEM as a percentage of CD45⁺ cells as analyzed by flow cytometry (>5 mice/group). F, orthotopic PyMT-derived tumors were grown to a median diameter of 1.0 cm, and tumor-bearing mice were administered intravenous paclitaxel (PTX; 10 mg/kg), and total tumor burden/animal assessed until endpoint. α IL4-neutralizing antibody was administered 1 day before chemotherapy (CTX) and then every 5 days for the duration of the study. Treatment schematic is depicted at top, and data are displayed as mean tumor burden \pm SEM (>5 mice/group). Statistical significance was determined by two-way ANOVA. G, orthotopic PyMT-derived tumors were implanted into syngeneic IL4R α -proficient (+/+) and -deficient (-/-) mice and grown to a median diameter of 1.0 cm. Mice were then treated with intravenous paclitaxel (10 mg/kg), and total tumor burden/animal assessed until endpoint. α CD8-depleting antibody was administered 1 day before chemotherapy and then every 5 days for the duration of the study. Treatment schematic is depicted at top, and data are displayed as mean tumor burden \pm SEM (>5 mice/group). Statistical significance was determined by two-way ANOVA. H, MMTV-PyMT transgenic mice were treated with α IL4 and/or α IL13 mAbs between 80 to 85 days of age, and 5 days later were treated with 10 mg/kg of paclitaxel as indicated. Tumor volume is shown as a relative change between the first dose of paclitaxel and 15 days later. Treatment schematic is depicted at top, and data are displayed as the mean \pm SEM (>6 mice/group). For all figures, statistical significance is shown as follows: *, $P < 0.05$; **, $P < 0.01$; ***, $P < 0.001$.

Shiao et al.

macrophages that recruit CD8⁺ T cells via increased expression of macrophage-derived chemokines (33), similar to results reported for radiation-induced pneumonitis implicating macrophage-derived CCL22 and CCL17 (ligands for CCR4; ref. 29). Depletion of CD4⁺ T cells or neutralization of the type 2 cytokines, i.e., IL4 or IL13 that they express, phenocopied CSF-1/CSF-1R blockade without depletion of macrophages. Improved responses to radiotherapy resulting from these treatments were dependent on the increased presence of CD8⁺ T cells in irradiated tumors as their selective depletion before radiotherapy abrogated the improved outcomes.

Based on subcutaneous xenograft models of head and neck cancer (34) and B16 melanoma (35), others have reported that high-dose radiotherapy leads to increased presence of CD11b⁺ myeloid cells that significantly affects outcome, as therapeutic use of CD11b-blocking mAbs or administration of clodronate liposomes restricted tumor regrowth associated with reduced myeloid-dependent angiogenesis (34, 36). Researchers from other studies in melanoma have reported that radiotherapy as monotherapy promotes CD8⁺ T-cell infiltration (35), and that CSF-1R blockade improves efficacy of adoptive T-cell transfer (18, 36). These results are in agreement with findings herein and elsewhere (16, 24, 33) that macrophages in tumor parenchyma limit CD8⁺ T-cell recruitment and effector function, and thereby restrict efficacy of cytotoxic therapies.

In mouse models of pancreatic neuroendocrine tumor growth, low-dose (2 Gy) radiotherapy improved efficacy of adoptive T-cell transfer by mechanisms involving repolarization of macrophages from expressing high levels of Ym-1 and Arginase-1 to instead expressing elevated inducible nitric oxide synthase, changes that correlated with enhanced recruitment of cytotoxic CD8⁺ T cells (28). Using 60-Gy doses, others have reported that focal radiotherapy induces expression of genes associated with T_H2-type macrophage activation (37, 38). In the mammary carcinoma model used herein, low-dose (2 Gy) radiotherapy alone was without consequence (data not shown), whereas 5-Gy focal radiotherapy led to enhanced expression of genes associated with both T_H1-type (*Il1a*, *Il1b*, *Tnfa*) and T_H2-type (*Cd163*, *Mrc1*, *Arg1*) macrophage activation. The polarization state of macrophages and other infiltrating cells is significant as blockade of IL4R α signaling similarly improved radiotherapy (and chemotherapy) response by CD8⁺ T-cell-dependent mechanisms. In human breast cancer, CD4⁺ T cells are biased toward production of IL4 and IL13 (39), a phenotype that is recapitulated in MMTV-PyMT transgenic mice (23). Although our results revealed that type 1 and 2 IL4/13 receptors were both broadly expressed by tumor-infiltrating stromal cells, it remains unclear whether IL4 directly or indirectly suppresses CD8⁺ T-cell recruitment/function. We favor the hypothesis that IL4 suppresses CD8⁺ T-cell activity indirectly through regulation of macrophage polarization, as we and others have reported (23, 40), and consistent with a role for macrophages in mediating resistance to radiotherapy and che-

motherapy. However, it is possible that IL4 directly suppresses CD8⁺ T-cell cytotoxic effector function (41), and in other tumor types, malignant cells also express IL4R α (42, 43).

Based on compelling preclinical data revealing improved responses to chemotherapy and delayed/slowed solid tumor growth following CSF-1R blockade (16, 17, 44, 45), clinical trials evaluating efficacy of CSF-1R antagonists in several types of solid tumors are ongoing (NCT01596751, NCT01349036, NCT01004861, and NCT01346358). Salient for translation to the clinic regarding macrophage repolarization versus depletion is the fact that whereas macrophage depletion before radiotherapy was without consequence, IL4 neutralization before radiotherapy yielded an improved outcome. Based on data herein that IL4 neutralization also improved response to chemotherapy, we assert that IL4 and/or IL13 neutralization represents a compelling immune-based strategy for improving responses in patients receiving either chemotherapy or radiotherapy.

Disclosure of Potential Conflicts of Interest

C.C. Park has ownership interest (including patents) in Oncosynergy. No potential conflicts of interest were disclosed by the other authors.

Authors' Contributions

Conception and design: S.L. Shiao, B. Ruffell, D.G. DeNardo, L.M. Coussens
Development of methodology: S.L. Shiao, B.A. Faddegon, C.C. Park, L.M. Coussens

Acquisition of data (provided animals, acquired and managed patients, provided facilities, etc.): S.L. Shiao, B. Ruffell, D.G. DeNardo, B.A. Faddegon, L.M. Coussens

Analysis and interpretation of data (e.g., statistical analysis, biostatistics, computational analysis): S.L. Shiao, B. Ruffell, D.G. DeNardo, B.A. Faddegon
Writing, review, and/or revision of the manuscript: S.L. Shiao, B. Ruffell, C.C. Park, L.M. Coussens

Study supervision: L.M. Coussens

Acknowledgments

The authors acknowledge technical and administrative support from Lidiya Korets, Kerry Fujikawa, Justin Tibbitts, Teresa Beechwood, Jo Hill, and Jane Wiesen, and helpful discussions from David M. Underhill. PLX3397 and the neutralizing IL13 mAb were generously provided by Plexikon Inc. and Gillian Kingsbury at Abbott Bioresearch Center, respectively.

Grant Support

The study was supported by the UCLA Clinical and Translational Science Institute and the American Society of Radiation Oncology (ASTRO, to S.L. Shiao), a grant from the NCI/NIH (to B. Ruffell), and grants from the NCI/NIH, the Department of Defense Breast Cancer Research Program (W81XWH-11-1-0702), the Susan G Komen Foundation (KG110560 and KG111084), and the Breast Cancer Research Foundation (to L.M. Coussens).

The costs of publication of this article were defrayed in part by the payment of page charges. This article must therefore be hereby marked *advertisement* in accordance with 18 U.S.C. Section 1734 solely to indicate this fact.

Received December 9, 2014; revised January 27, 2015; accepted January 29, 2015; published OnlineFirst February 25, 2015.

References

- Jemal A. Global burden of cancer: opportunities for prevention. *Lancet* 2012;380:1797–9.
- Fleming ST, Kimmick GG, Sabatino SA, Cress RD, Wu XC, Trentham-Dietz A, et al. Defining care provided for breast cancer based on medical record review

or Medicare claims: information from the Centers for Disease Control and Prevention Patterns of Care Study. *Ann Epidemiol* 2012;22:807–13.

- Formenti SC, Demaria S. Combining radiotherapy and cancer immunotherapy: a paradigm shift. *J Natl Cancer Inst* 2013;105:256–65.

4. Ma J, Liu L, Che G, Yu N, Dai F, You Z. The M1 form of tumor-associated macrophages in non-small cell lung cancer is positively associated with survival time. *BMC Cancer* 2010;10:112.
5. Shiao SL, Coussens LM. The tumor-immune microenvironment and response to radiation therapy. *J Mammary Gland Biol Neoplasia* 2010;15:411–21.
6. Shiao SL, Ganessan AP, Rugo HS, Coussens LM. Immune microenvironments in solid tumors: new targets for therapy. *Genes Dev* 2011;15:2559–72.
7. Ruffell B, Affara NI, Coussens LM. Differential macrophage programming in the tumor microenvironment. *Trends Immunol* 2012;33:119–25.
8. Bingle L, Brown NJ, Lewis CE. The role of tumour-associated macrophages in tumour progression: implications for new anticancer therapies. *J Pathol* 2002;196:254–65.
9. Pollard JW. Trophic macrophages in development and disease. *Nat Rev Immunol* 2009;9:259–70.
10. Qian BZ, Pollard JW. Macrophage diversity enhances tumor progression and metastasis. *Cell* 2010;141:39–51.
11. Burt BM, Rodig SJ, Tillemann TR, Elbardissi AW, Bueno R, Sugarbaker DJ. Circulating and tumor-infiltrating myeloid cells predict survival in human pleural mesothelioma. *Cancer* 2011;117:5234–44.
12. Tang R, Beuvon F, Ojeda M, Mosseri V, Pouillart P, Scholl S. M-CSF (monocyte colony stimulating factor) and M-CSF receptor expression by breast tumour cells: M-CSF mediated recruitment of tumour infiltrating monocytes? *J Cell Biochem* 1992;50:350–6.
13. Beck AH, Espinosa I, Edris B, Li R, Montgomery K, Zhu S, et al. The macrophage colony-stimulating factor 1 response signature in breast carcinoma. *Clin Cancer Res* 2009;15:778–87.
14. Campbell MJ, Tonlaar NY, Garwood ER, Huo D, Moore DH, Khrantsov AI, et al. Proliferating macrophages associated with high grade, hormone receptor negative breast cancer and poor clinical outcome. *Breast Cancer Res Treat* 2011;128:703–11.
15. Sharma M, Beck AH, Webster JA, Espinosa I, Montgomery K, Varma S, et al. Analysis of stromal signatures in the tumor microenvironment of ductal carcinoma in situ. *Breast Cancer Res Treat* 2010;123:397–404.
16. DeNardo DG, Brennan DJ, Rexhepaj E, Ruffell B, Shiao SL, Madden SF, et al. Leukocyte complexity predicts breast cancer survival and functionally regulates response to chemotherapy. *Cancer Discov* 2011;1:54–67.
17. Strachan DC, Ruffell B, Oei Y, Bissell MJ, Coussens LM, Pryer N, et al. CSF1R inhibition delays cervical and mammary tumor growth in murine models by attenuating the turnover of tumor-associated macrophages and enhancing infiltration by CD8 T cells. *Oncoimmunology* 2013;2:e26968.
18. Mok S, Koya RC, Tsui C, Xu J, Robert L, Wu L, et al. Inhibition of CSF-1 receptor improves the antitumor efficacy of adoptive cell transfer immunotherapy. *Cancer Res* 2014;74:153–61.
19. Xu J, Escamilla J, Mok S, David J, Priceman S, West B, et al. CSF1R signaling blockade stanches tumor-infiltrating myeloid cells and improves the efficacy of radiotherapy in prostate cancer. *Cancer Res* 2013;73:2782–94.
20. Mitchem JB, Brennan DJ, Knolhoff BL, Belt BA, Zhu Y, Sanford DE, et al. Targeting tumor-infiltrating macrophages decreases tumor-initiating cells, relieves immunosuppression, and improves chemotherapeutic responses. *Cancer Res* 2013;73:1128–41.
21. Lin EY, Nguyen AV, Russell RG, Pollard JW. Colony-stimulating factor 1 promotes progression of mammary tumors to malignancy. *J Exp Med* 2001;193:727–40.
22. Qian BZ, Li J, Zhang H, Kitamura T, Zhang J, Campion LR, et al. CCL2 recruits inflammatory monocytes to facilitate breast-tumour metastasis. *Nature* 2011;475:222–5.
23. DeNardo DG, Barreto JB, Andreu P, Vasquez L, Tawfik D, Kolhatkar N, et al. CD4(+) T cells regulate pulmonary metastasis of mammary carcinomas by enhancing protumor properties of macrophages. *Cancer Cell* 2009;16:91–102.
24. Ruffell B, Chang-Strachan D, Chan V, Rosenbusch A, Ho CMT, Pryer N, et al. Macrophage IL-10 blocks CD8(+) T cell-dependent responses to chemotherapy by suppressing IL-12 expression in intratumoral dendritic cells. *Cancer Cell* 2014;26:623–37.
25. Guy CT, Cardiff RD, Muller WJ. Induction of mammary tumors by expression of polyomavirus middle T oncogene: a transgenic mouse model for metastatic disease. *Mol Cell Biol* 1992;12:954–61.
26. West B, Denardo D, Tsai J, Hann B, Nguyen H, Wong B, et al. Efficacy of the selective CSF-1R kinase inhibitor PLX3397 in mouse models of tumor growth and bone metastasis (Abstract nr 3850). Washington, DC: AACR; 2010. p. 7864.
27. Anthony SP, Puzanov I, Lin PS, Nolop KB, West B, Von Hof DD. Pharmacodynamic activity demonstrated in phase I for PLX3397, a selective inhibitor of FMS and Kit. *J Clin Oncol* 2011;29:abstr 3093.
28. Klug F, Prakash H, Huber PE, Seibel T, Bender N, Halama N, et al. Low-dose irradiation programs macrophage differentiation to an iNOS(+)/M1 phenotype that orchestrates effective T cell immunotherapy. *Cancer Cell* 2013;24:589–602.
29. Inoue T, Fujishima S, Ikeda E, Yoshie O, Tsukamoto N, Aiso S, et al. CCL22 and CCL17 in rat radiation pneumonitis and in human idiopathic pulmonary fibrosis. *Eur Respir J* 2004;24:49–56.
30. Wills-Karp M, Finkelman FD. Untangling the complex web of IL-4- and IL-13-mediated signaling pathways. *Sci Signal* 2008;1:pe55.
31. Movahedi K, Laoui D, Gysmans C, Baeten M, Stange G, Van den Bossche J, et al. Different tumor microenvironments contain functionally distinct subsets of macrophages derived from Ly6C(high) monocytes. *Cancer Res* 2010;70:5728–39.
32. Ruffell B, Au A, Rugo HS, Esserman LJ, Hwang ES, Coussens LM. Leukocyte composition of human breast cancer. *Proc Natl Acad Sci U S A* 2012;109:2796–801.
33. Affara NI, Ruffell B, Medler TR, Gunderson AJ, Johansson M, Bornstein S, et al. B cells regulate macrophage phenotype and response to chemotherapy in squamous carcinomas. *Cancer Cell* 2014;25:809–21.
34. Ahn GO, Tseng D, Liao CH, Dorie MJ, Czechowicz A, Brown JM. Inhibition of Mac-1 (CD11b/CD18) enhances tumor response to radiation by reducing myeloid cell recruitment. *Proc Natl Acad Sci U S A* 2010;107:8363–8.
35. Lugade AA, Moran JP, Gerber SA, Rose RC, Frelinger JG, Lord EM. Local radiation therapy of B16 melanoma tumors increases the generation of tumor antigen-specific effector cells that traffic to the tumor. *J Immunol* 2005;174:7516–23.
36. Meng Y, Beckett MA, Liang H, Mauceri HJ, van Rooijen N, Cohen KS, et al. Blockade of tumor necrosis factor alpha signaling in tumor-associated macrophages as a radiosensitizing strategy. *Cancer Res* 2010;70:1534–43.
37. Crittenden MR, Savage T, Cottam B, Baird J, Rodriguez PC, Newell P, et al. Expression of arginase 1 in myeloid cells limits control of residual disease after radiation therapy of tumors in mice. *Radiat Res* 2014;182:182–90.
38. Crittenden MR, Cottam B, Savage T, Nguyen C, Newell P, Gough MJ. Expression of NF-kappaB p50 in tumor stroma limits the control of tumors by radiation therapy. *PLoS One* 2012;7:e39295.
39. Pedroza-Gonzalez A, Xu K, Wu TC, Aspord C, Tindle S, Marches F, et al. Thymic stromal lymphopoietin fosters human breast tumor growth by promoting type 2 inflammation. *J Exp Med* 2011;208:479–90.
40. Gocheva V, Wang HW, Gadea BB, Shree T, Hunter KE, Garfall AL, et al. IL-4 induces cathepsin protease activity in tumor-associated macrophages to promote cancer growth and invasion. *Genes Dev* 2010;24:241–55.
41. Kemp RA, Ronchese F. Tumor-specific Tc1, but not Tc2, cells deliver protective antitumor immunity. *J Immunol* 2001;167:6497–502.
42. Burt BM, Bader A, Winter D, Rodig SJ, Bueno R, Sugarbaker DJ. Expression of interleukin-4 receptor alpha in human pleural mesothelioma is associated with poor survival and promotion of tumor inflammation. *Clin Cancer Res* 2012;18:1568–77.
43. Venmar KT, Carter KJ, Hwang DG, Dozier EA, Fingleton B. IL4 receptor ILR4alpha regulates metastatic colonization by mammary tumors through multiple signaling pathways. *Cancer Res* 2014;74:4329–40.
44. Pyonteck SM, Akkari L, Schuhmacher AJ, Bowman RL, Sevenich L, Quail DF, et al. CSF-1R inhibition alters macrophage polarization and blocks glioma progression. *Nat Med* 2013;19:1264–72.
45. Ries CH, Cannarile MA, Hoves S, Benz J, Wartha K, Runza V, et al. Targeting tumor-associated macrophages with anti-CSF-1R antibody reveals a strategy for cancer therapy. *Cancer Cell* 2014;25:846–59.

Cancer Immunology Research

T_H2-Polarized CD4⁺ T Cells and Macrophages Limit Efficacy of Radiotherapy

Stephen L. Shiao, Brian Ruffell, David G. DeNardo, et al.

Cancer Immunol Res 2015;3:518-525. Published OnlineFirst February 25, 2015.

Updated version	Access the most recent version of this article at: doi: 10.1158/2326-6066.CIR-14-0232
Supplementary Material	Access the most recent supplemental material at: http://cancerimmunolres.aacrjournals.org/content/suppl/2015/02/26/2326-6066.CIR-14-0232.DC1.html

Cited Articles	This article cites by 43 articles, 20 of which you can access for free at: http://cancerimmunolres.aacrjournals.org/content/3/5/518.full.html#ref-list-1
-----------------------	---

E-mail alerts	Sign up to receive free email-alerts related to this article or journal.
----------------------	--

Reprints and Subscriptions	To order reprints of this article or to subscribe to the journal, contact the AACR Publications Department at pubs@aacr.org .
-----------------------------------	--

Permissions	To request permission to re-use all or part of this article, contact the AACR Publications Department at permissions@aacr.org .
--------------------	---

T_H2-polarized CD4⁺ T cells and macrophages limit efficacy of radiation therapy

Supplemental Data

Stephen L. Shiao¹, Brian Ruffell², David G. DeNardo³, Bruce A. Faddegon⁴, Catherine C. Park⁴, Lisa M. Coussens^{2,*}

¹Department of Radiation Oncology, Cedars-Sinai Medical Center, Los Angeles, CA 90048

²Department of Cell, Developmental & Cancer Biology and Knight Cancer Institute, Oregon Health & Science University, Portland, OR

³Department of Medicine, Department of Pathology and Immunology, and Siteman Cancer Center, Washington University School of Medicine, St Louis, MO 63110.

⁴Department of Radiation Oncology, Helen Diller Family Comprehensive Cancer Center, University of California, San Francisco, San Francisco, CA 94143

*Address for correspondence:

Lisa M. Coussens, Ph.D.

Cell, Developmental & Cancer Biology

Knight Cancer Institute

Oregon Health & Science University

3181 SW Sam Jackson Park Road

Portland, OR 97239-3098

Voice: 503-494-7811

Fax: 503-494-4253

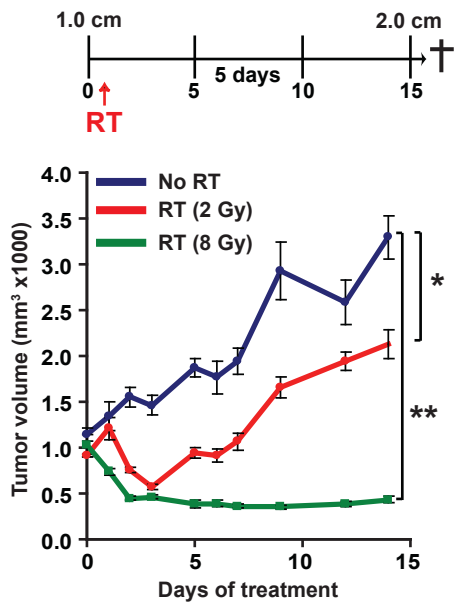
email: coussenl@ohsu.edu

Supplemental Figure Legends

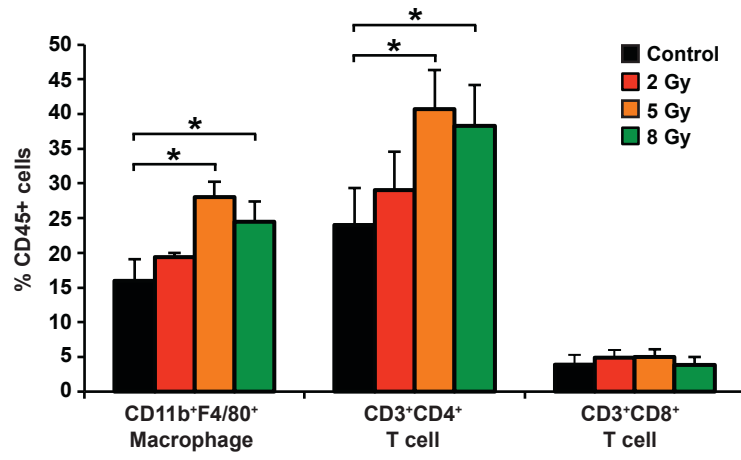
Supplemental Figure 1: Radiation dose response and immune profile. **A)** Orthotopic MMTV-PyMT-derived explant tumors were grown to a median diameter of 1.0 cm for study enrollment (day 0), and one day later received localized gamma irradiation (2 or 8 Gy). Total tumor burden/animal was then assessed every 3 days until endpoint. Treatment schematic is depicted at top and data are displayed as mean tumor burden \pm SEM (>5 mice/group). Significance was determined by two-way ANOVA. One of two experiments is shown. **B)** Number of CD3⁺CD4⁺, CD3⁺CD8⁺, and CD11b⁺F4/80⁺ cells within tumors 14 days following RT in groups that were untreated, treated with RT (2 Gy), RT (5 Gy) or RT (8 Gy). Data are depicted as mean number of cells \pm SEM as a % of CD45⁺ cells as analyzed by flow cytometry (>5 mice/group). Significance was determined by an unpaired t-test relative to untreated controls. For all panels, significance is shown as *p < 0.05, **p < 0.01, ***p < 0.001.

Supplemental Figure 2: Immune profile with RT in combination with α CSF-1 mAb or PLX3397. **A)** Number of CD3⁺CD4⁺, CD3⁺CD8⁺, and CD11b⁺F4/80⁺ cells within tumors 4 days following RT (2 days after administration of α CSF-1 mAb) in groups that were untreated, treated with α CSF-1 mAb alone, RT (5 Gy) alone or treated with a combination of RT and α CSF-1 mAb. **B)** Number of CD3⁺CD4⁺, CD3⁺CD8⁺, and CD11b⁺F4/80⁺ cells within tumors 4 days following RT (2 days after administration of PLX3397) in groups that were untreated, treated with PLX3397 alone, RT (5 Gy) alone or treated with a combination of RT and PLX3397. Data are depicted as mean number of cells \pm SEM as a % of CD45⁺ cells as analyzed by flow cytometry (>5 mice/group). For all figures significance is shown as *p < 0.05, **p < 0.01, ***p < 0.001.

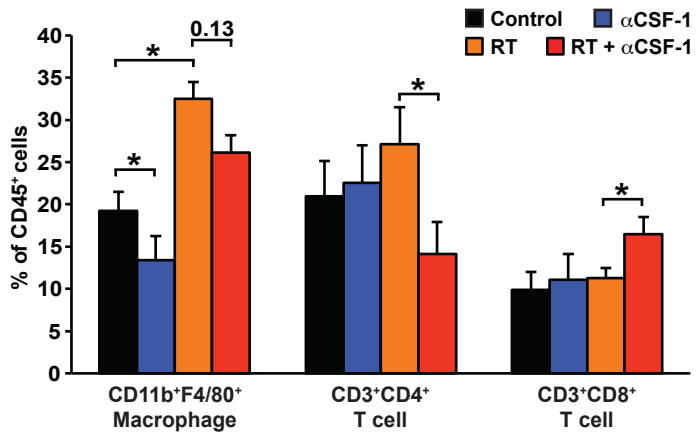
A



B



A



B

